Electronic Supplementary Information for:

Fluorescent graphene quantum dots-enhanced machine learning for accurate detection and quantification of Hg^{2+} and Fe^{3+} in real water samples.

Mauricio Llaver,[a,*] Santiago D. Barrionuevo,[b] Jorge M. Núñez,[c,d,e,f,g] Agostina L. Chapana,[a] Rodolfo G. Wuilloud,[a] Myriam H. Aguirre[f,g,h] and Francisco J. Ibañez[b,*]

[a] *Laboratorio de Química Analítica para Investigación y Desarrollo (QUIANID), Facultad de Ciencias Exactas y Naturales, Universidad Nacional de Cuyo / Instituto Interdisciplinario de Ciencias Básicas (ICB), CONICET UNCUYO, Padre J. Contreras 1300, (5500) Mendoza, Argentina.*

[b] *Instituto de Investigaciones Fisicoquímicas, Teóricas y Aplicadas (INIFTA). Universidad Nacional de La Plata - CONICET. Sucursal 4 Casilla de Correo 16 (1900) La Plata, Argentina.*

[c] *Resonancias Magnéticas-Centro Atómico Bariloche (CNEA, CONICET), S. C. Bariloche 8400, Río Negro, Argentina.*

[d] *Instituto de Nanociencia y Nanotecnología, CNEA, CONICET, S. C. Bariloche 8400, Río Negro, Argentina.*

[e] *Instituto Balseiro (UNCUYO, CNEA), Av. Bustillo 9500, S.C. de Bariloche 8400, Río Negro, Argentina.*

[f] *Instituto de Nanociencia y Materiales de Aragón, CSIC-Universidad de Zaragoza, C/ Pedro Cerbuna 12, 50009, Zaragoza, Spain.*

[g] *Laboratorio de Microscopías Avanzadas, Universidad de Zaragoza, Mariano Esquillor s/n, 50018, Zaragoza, Spain.*

[h] *Dpto. de Física de la Materia Condensada, Universidad de Zaragoza, C/ Pedro Cerbuna 12, 50009, Zaragoza, Spain.*

e-mail: mllaver@mendoza-conicet.gob.ar
e-mail: fjiban@inifta.unlp.edu.ar

S1. The output files from the experimental obtention of the excitation-emission matrices (EEMs) with known Hg^{2+} and Fe^{3+} concentrations had to be pre-processed prior to the application of the machine learning models used for the prediction of analyte concentrations in real samples.

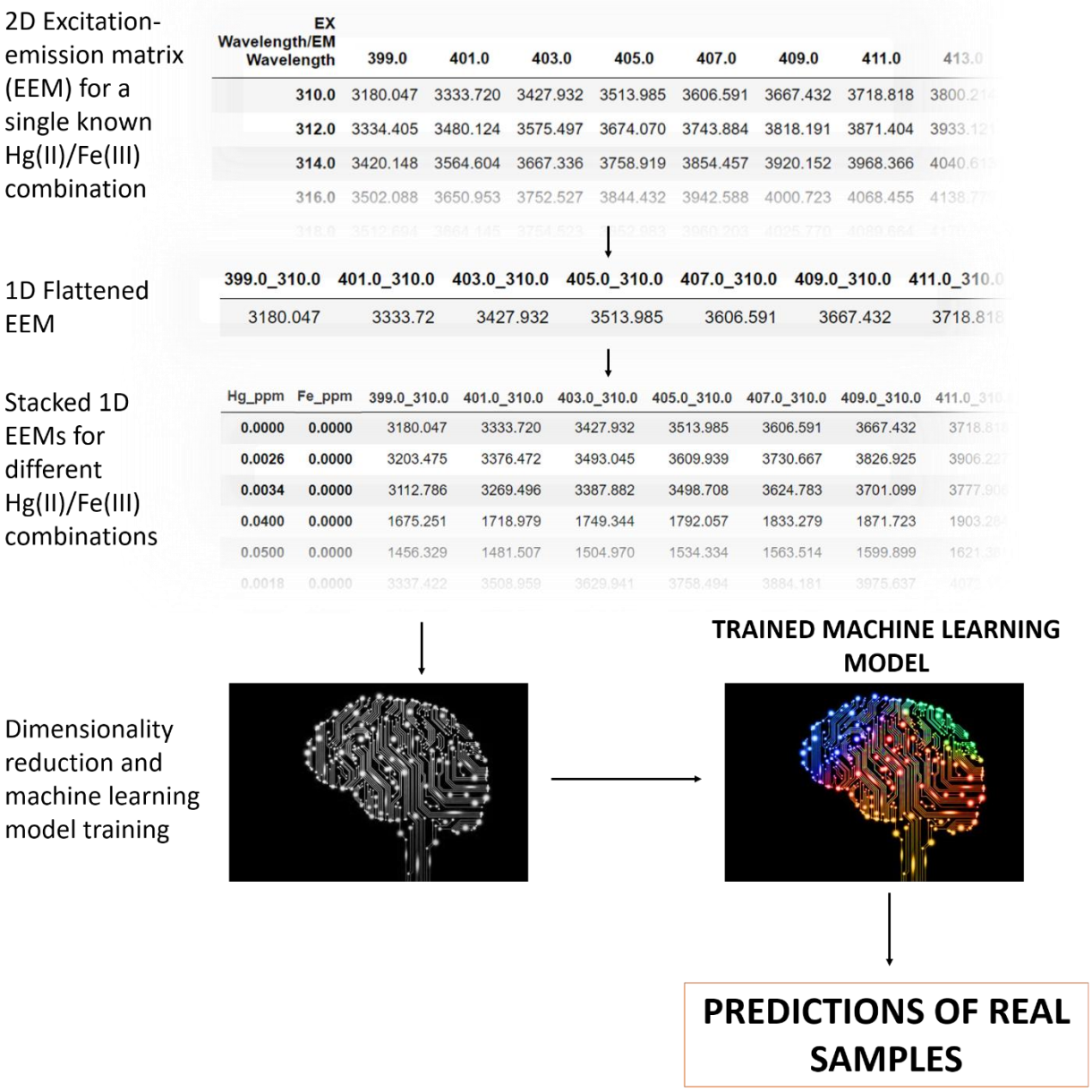

Figure S1. Schematic representation of the data handling process.

S2. Additional XPS. To complement the characterization of the urea-modified graphene quantum dots (uGQDs) and 1-nitroso-2-naphthol-modified NN-uGQDs, X-ray photoelectron spectra of pristine 1-nitroso-2-naphthol (NN).

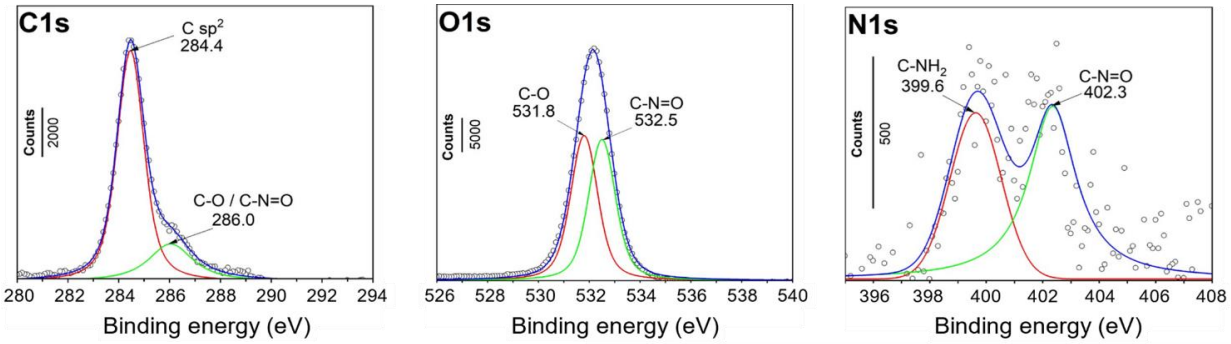

Figure S2. Top: C 1s, O 1s and N 1s XPS spectra for pristine NN, including the deconvolution of the instrumental signal.

S3. Excitation Emission Matrix (EMM) for GQDs synthesized without urea. The EMMs for graphene quantum dots (GQDs) synthesized without urea, as control, show similarities with that of urea-modified graphene quantum dots. The main difference between both cases is the EMM observed for uGQDs with an excitation wavelength of 315 nm, which is not presence in the case of GQDs.

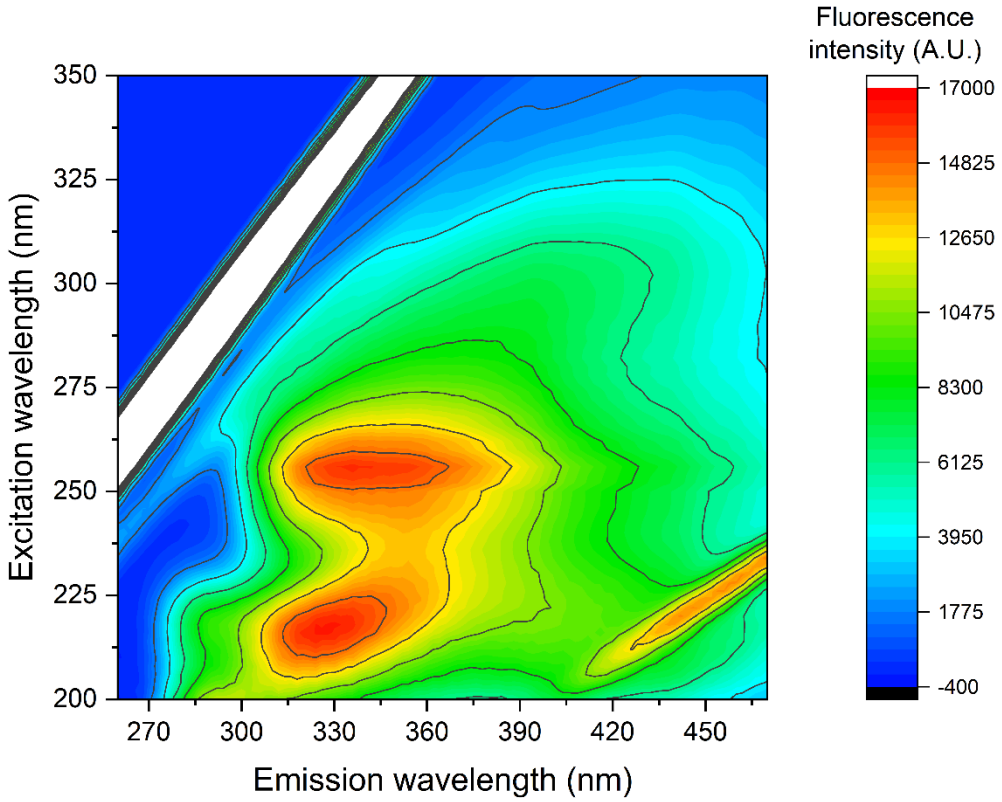

Figure S3. Excitation-emission matrix (EMM) for as-synthesized graphene quantum dots. The main high-intensity emission resulting from scattering (when $\lambda_{exc} = \lambda_{em}$) has been whitened to improve visualization.

S4. The EMMs of 1-nitroso-2-naphthol-modified nitrogenated graphene quantum dots (NN-uGQDs), in the presence of 0.20 mg L^{-1} of both Hg^{2+} and Fe^{3+}, show significant differences in the emission profile. These differences were key for the application of the developed machine learning model, used for the simultaneous prediction of Hg^{2+} and Fe^{3+} concentrations in unknown samples.

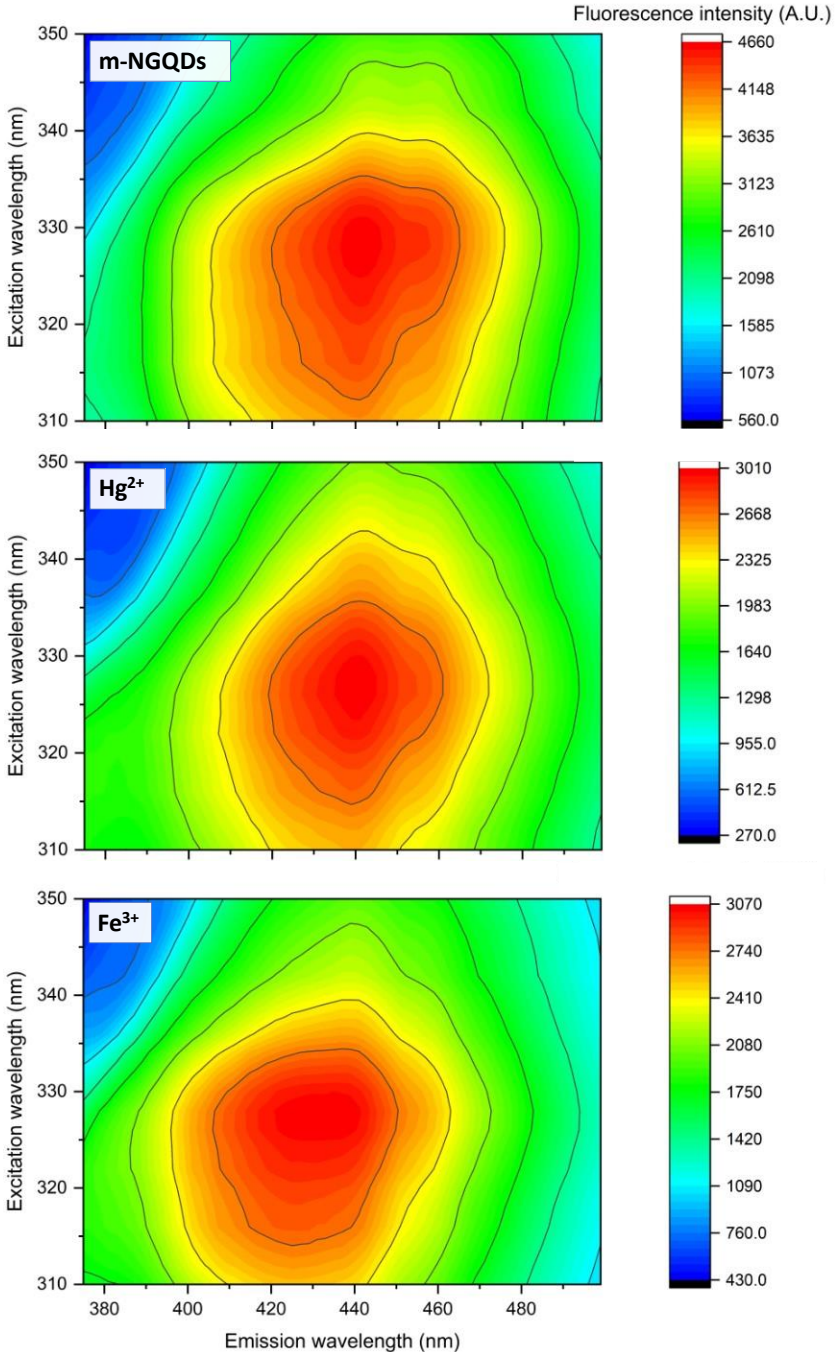

Figure S4. EMM spectra for 1-nitroso-2-naphthol-modified nitrogenated graphene quantum dots before (m-NGQDs, shown on top) and after the addition of 0.20 mg L^{-1} of Hg^{2+} (middle) and Fe^{3+} (bottom).

S5. Response time. The response time of the probe differed for the studied analytes, having Hg^{2+} and immediate effect on the emission, while Fe^{3+} took 15 min to produce its full quenching effect.

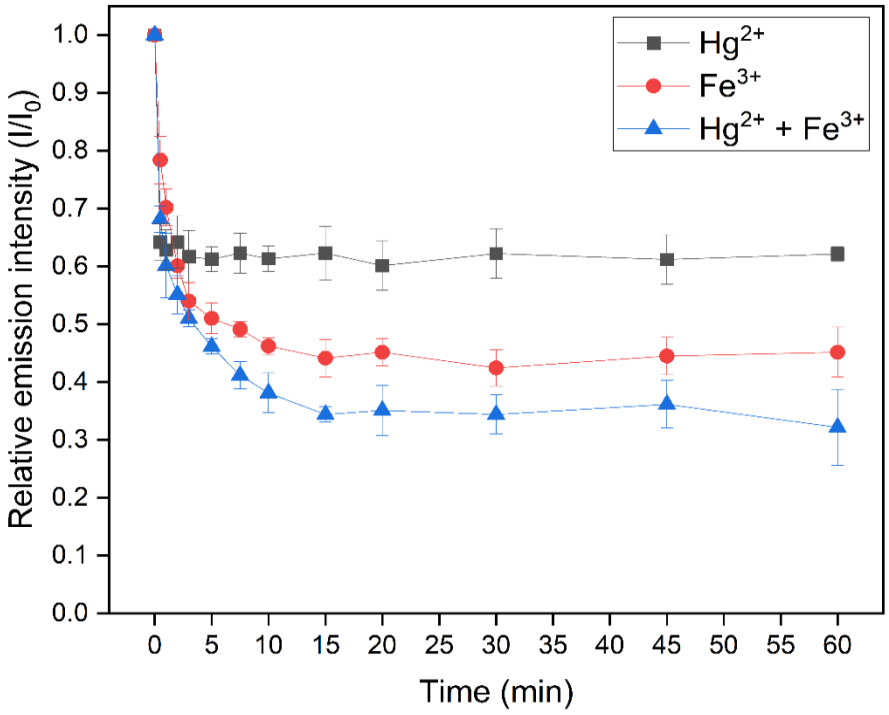

Figure S5. Relative EMM intensity of 1-nitroso-2-naphthol-functionalized N-doped graphene quantum dots as a function of time after the addition of 0.35 mg mL^{-1} of Hg^{2+}, 0.50 mg mL^{-1} Fe^{3+} and 0.35 mg mL^{-1} of Hg^{2+} + 0.50 mg mL^{-1} Fe^{3+}. The spectra taken at time = 0 has been considered as the reference emission intensity (I_0) and n = 3.

S6. Table comparing different Fluorescent Sensors

Table S1. Comparison of the hereby presented results with other recently published GQD-based fluorescence sensors for Hg^{2+} and Fe^{3+} determination.

Fluorescence Sensor	*Synthesis method*	*Linear range*	*LOD*		*Real Samples*	*Reference*
			Hg^{2+}	*Fe^{3+}*		
Glutathione-doped GQDs	Pyrolysis	1-150 μM	-	0.10 μM	Drinking water	[1]
N-doped GQDs	Hydrothermal	0-30 μM	0.25nM	-	River water	[2]
P, N-doped GQDs	Pyrolysis	Not reported	0.13 μM	-	Natural spring wáter, river wáter and serum sample	[3]
GQDs	Pyrolysis	0–60 nM	-	0.024 nM	Drinking water	[4]
NN-u-GQDs	Electrochemical exfoliation from 3D graphene	0-0.02 μM 0-0.08 μM	0.005 μM	0.017 μM	Tap water, river wáter and dam wáter	This work

S7. Instrumental conditions for the determination of Hg^{2+} in water samples by cold vapor-atomic fluorescence spectrometry. All measurements were carried out on samples that were previously acidified with HNO_3 up to a final concentration of 1.0 mol L^{-1}. The calibration curve was obtained using standard samples prepared in 1.0 mol L^{-1} HNO_3. On the other hand, the spectrophotometric method used for Fe^{3+} determination was based on a liquid-liquid extraction using ethyl acetate, after addition of KSCN as complexing and chromogenic reagent.

Table S2. Instrumental conditions for the determination of Hg^{2+} in water samples by cold vapor-atomic fluorescence spectrometry.

AFS instrumental conditions	
Wavelength	257.3 nm
Measurement mode	Peak height
Primary lamp current	8.0 mA
Atomizer temperature	300 ºC
Boost current	0
PMT voltage	240 V
Cold vapor generation conditions	
Sample volume	2.0 mL
Carrier	1.0 mol L^{-1} HNO_3
Carrier flow rate	4.0 mL min^{-1}
Reductant	0.5% (w/v) $NaBH_4$
Reductant flow rate	4.0 mL min^{-1}
Carrier gas and flow rate	Ar, 500 mL min^{-1}

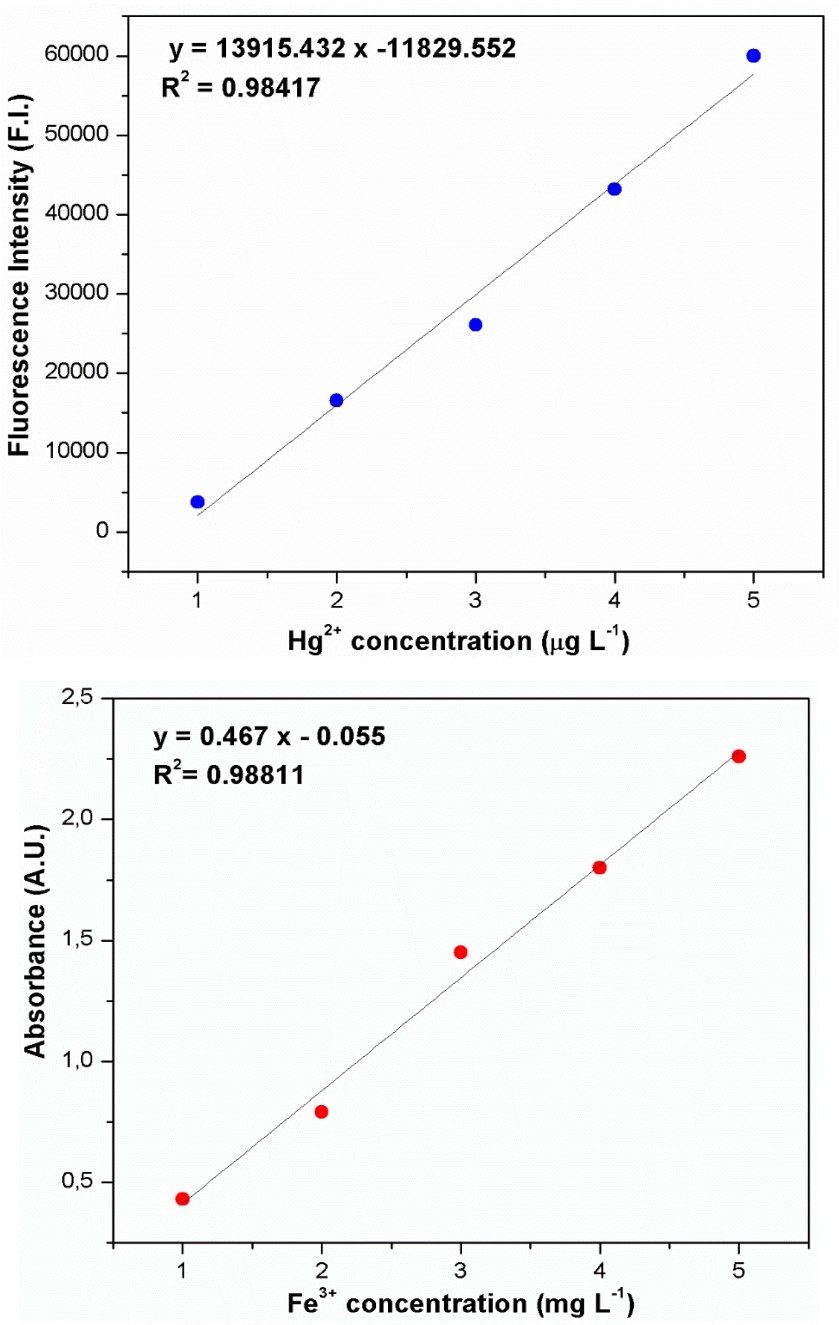

Figure S6. Calibration curves for Hg^{2+} (above) and Fe^{3+} (below) are presented, corresponding to the spectrophotometric and CV-AFS measurements utilized in the validation process.

References

(1) Saenwong, K.; Nuengmatcha, P.; Sricharoen, P.; Limchoowong, N.; Chanthai, S. GSH-Doped GQDs Using Citric Acid Rich-Lime Oil Extract for Highly Selective and Sensitive Determination and Discrimination of Fe3+ and Fe2+ in the Presence of H2O2 by a Fluorescence "Turn-off" Sensor. *RSC Advances* **2018**, *8* (18), 10148–10157. https://doi.org/10.1039/c7ra13432k.

(2) Xiong, Z.; Zou, Y.; Cao, X.; Lin, Z. Color-Tunable Fluorescent Nitrogen-Doped Graphene Quantum Dots Derived from Pineapple Leaf Fiber Biomass to Detect Hg2+. *Chinese Journal of Analytical Chemistry* **2022**, *50* (2), 69–76. https://doi.org/10.1016/j.cjac.2021.10.003.

(3) Şenol, A. M.; Kassa, S. B.; Onganer, Y. A Simple Fluorescent "Turn off-on" Sensor Based on P, N-Doped Graphene Quantum Dots for Hg2+ and Cysteine Determination. *Sensors and Actuators A: Physical* **2023**, *356*, 114362. https://doi.org/10.1016/j.sna.2023.114362.

(4) Mandal, D.; De, P.; Khatun, S.; Gupta, A. N.; Chandra, A. Highly Fluorescent Graphene Quantum Dots as "Turn off–on" Nanosensor for Detecting Toxic Metal Ions to Organic Pollutant. *Int. J. Environ. Sci. Technol.* **2024**, *21* (2), 1637–1648. https://doi.org/10.1007/s13762-023-05033-1.